Dalton Transactions

PAPER

View Article Online
View Journal | View Issue

Cite this: *Dalton Trans.*, 2019, **48**, 17840

Half-sandwich rare-earth metal complexes bearing a C_5Me_4-C_6H_4-*o*-CH_2NMe_2 ligand: synthesis, characterization and catalytic properties for isoprene, 1-hexene and MMA polymerization†

Tingting Song, Ning Liu, Xiaobo Tong, Feng Li, Xiaoyue Mu* and Ying Mu *

Received 14th October 2019,
Accepted 18th November 2019

DOI: 10.1039/c9dt04029c

rsc.li/dalton

A new *ortho*-dimethylaminomethylphenyl-tetramethylcyclopentadienyl ligand C_5Me_4H-C_6H_4-*o*-CH_2NMe_2 (H**L**) and a series of rare-earth metal complexes bearing this ligand were synthesized. Of these complexes, two binuclear alkyl complexes $[(C_5Me_4$-C_6H_4-*o*-$CH_2N(Me)CH_2$-μ$)Ln(CH_2SiMe_3)]_2$ (Ln = Sc (**1a**) and Y (**1b**)) were obtained from the alkane elimination reaction of the free ligand with $Ln(CH_2SiMe_3)_3(THF)_2$, followed by an intramolecular C–H activation process of a NMe group in the ligand with a CH_2SiMe_3 group, two binuclear dichloro complexes $(C_5Me_4$-C_6H_4-*o*-$CH_2NMe_2)_2Y_2Cl_4[LiCl(THF)_2]$ (**2a**) and $[(C_5Me_4$-C_6H_4-*o*-$CH_2NMe_2)LuCl($μ-Cl$)]_2$ (**2b**) were synthesized by the reaction of anhydrous yttrium or lutetium trichloride with the lithium salt of the ligand Li**L**, and the binuclear bis(borohydrido) complexes $[(C_5Me_4$-C_6H_4-*o*-$CH_2NMe_2)Ln($μ-$BH_4)BH_4]_2$ (Ln = Sm (**3a**) and Nd (**3b**)) were synthesized by the reaction of $Ln(BH_4)_3(THF)_3$ (Ln = Sm and Nd) with the lithium salt of the ligand. The molecular structures of all complexes **1a**, **1b**, **2a**, **2b**, **3a** and **3b** were determined by single-crystal X-ray crystallography. Upon activation with $AlR_3/Ph_3CB(C_6F_5)_4$, MAO or MMAO, the binuclear alkyl complexes **1a** and **1b** show good catalytic activity for isoprene *cis*-1,4 enriched regioselective polymerization and moderate catalytic activity for 1-hexene polymerization. Complexes **3a** and **3b** were studied as catalysts for methyl methacrylate polymerization reaction under different conditions and were found to show moderate to high catalytic activity.

Introduction

In the past decades, the rare-earth metal complexes have received intensive attention in the field of catalytic olefin polymerization reactions and related catalytic transformations owing to their good performance in various catalytic processes.[1] Of the reported rare-earth metal complexes, a number of rare-earth-metal metallocene complexes bearing cyclopentadienyl ligand(s) with ancillary coordination group(s) have been exploited as catalysts for olefin polymerization reactions and a variety of related transformations.[2] Among these studies, considerable attention has been directed towards half-sandwich rare-earth metal complexes bearing one cyclopentadienyl ligand because such complexes are considered to provide a sterically and electronically more unsaturated metal center and thus expected to show unique reactivities differing from those of the metallocenes bearing two cyclopentadienyl ligands.[3] So far, some alkyl, hydrido, and amido half-sandwich rare-earth metal complexes and their cationic derivatives have been found to show unique catalytic potential in olefin polymerization reactions.[4–15] Hou *et al.* have reported the first isospecific 3,4-polymerization (100% 3,4; *mmmm* >99%) of isoprene by using binuclear silylene-linked cyclopentadienyl-phosphido rare earth metal alkyl complexes.[5a] They have also found that the half-sandwich dialkyl scandium complex with a coordinated ether side arm $(C_5Me_4C_6H_4OMe$-*o*$)Sc(CH_2SiMe_3)_2$ prefers to catalyze the *trans*-1,4-selective polymerization of isoprene (60–79%) while the phosphine analogue $[(C_5Me_4CH_2CH_2PPh_2)Sc(CH_2SiMe_3)_2]$ shows high *cis*-1,4 selectivity (84–90%) for the polymerization of isoprene under the same conditions. In contrast, the binuclear complex $[(C_5Me_4$-C_6H_4-*o*-$N(Me)CH_2$-μ$)Sc(CH_2SiMe_3)]_2$ shows only very low catalytic activity for the isoprene *cis*-1,4-selective polymerization.[5b] Our group has reported a number of new C_s-symmetric imino–cyclopentadienyl half sandwich scandium(III) complexes and found that they exhibit moderate catalytic

The State Key Laboratory for Supramolecular Structure and Materials, School of Chemistry, Jilin University, 2699 Qianjin Street, Changchun 130012, People's Republic of China. E-mail: xymu@jlu.edu.cn, ymu@jlu.edu.cn

†Electronic supplementary information (ESI) available: NMR spectra for the ligand, metal complexes, reaction mixtures of complex **1a**/$Ph_3CB(C_6F_5)_4$ and complex **1a**/$Al^iBu_3/Ph_3CB(C_6F_5)_4$, and the polymers, and crystal data and structure refinements. CCDC 1955350, 1955352, 1955355, 1955356, 1955359 and 1955360. For ESI and crystallographic data in CIF or other electronic format see DOI: 10.1039/C9DT04029C

activity for 1-hexene polymerization and produce high molecular weight isotactic poly(1-hexene) upon activation with $Al^iBu_3/Ph_3CB(C_6F_5)_4$ or MAO.[6] Cui *et al.* have previously studied a series of rare earth metal complexes chelated by an aminophenyl-functionalized-cyclopentadienyl ligand $[C_5Me_4\text{-}C_6H_4\text{-}o\text{-}NMe_2]^-$ and found that their borohydrido complexes exhibit high catalytic activity and specific selectivity in the polymerization of MMA while their chloro complexes are completely inactive.[9] Similar monocyclopentadienyl rare-earth metal borohydride complexes have also been developed and studied as catalysts for the polymerization of styrene, isoprene and MMA, as well as the copolymerization of isoprene with styrene.[16–24] To develop more and better half-sandwich rare-earth metal catalysts for olefin polymerization reactions, we have synthesized a number of new alkyl, chloro and borohydrido complexes of rare-earth metal complexes bearing a 2-(tetramethylcyclopentadienyl) benzylamido ligand $[C_5Me_4\text{-}C_6H_4\text{-}o\text{-}CH_2NMe_2]^-$, and found that these complexes show good catalytic performance for the polymerization reactions of isoprene, 1-hexene and MMA. We herein report the synthesis and structural characterization of these rare-earth metal alkyl, chloro and borohydrido complexes, and studies on their catalytic properties for the polymerization reactions of isoprene, 1-hexene and MMA.

Results and discussion

Synthesis and characterization of the free ligand (HL)

The new free ligand $C_5Me_4H\text{-}C_6H_4\text{-}o\text{-}CH_2NMe_2$ (**HL**) was synthesised by a convenient procedure as outlined in Scheme 1.

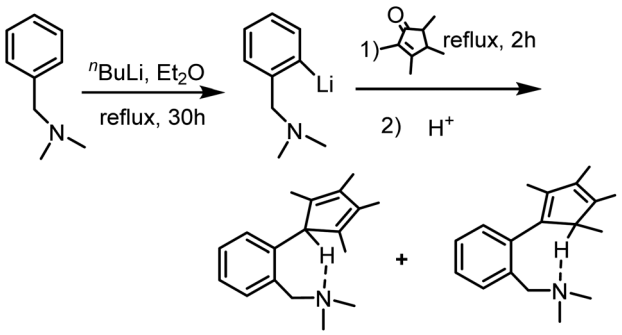

Scheme 1 Synthesis of the free ligand HL.

Ortholithiation of *N*,*N*-dimethylbenzylamine according to a literature procedure, followed by a nucleophilic addition reaction with 2,3,4,5-tetramethylcyclopentenone, an acidic workup, and a final distillation under reduced pressure gave the free ligand as a yellow viscous liquid in a reasonable yield (55%). The ^{1}H NMR spectrum is somewhat complicated due to a C–H···N hydrogen bond interaction between the acidic H atom of the Cp ring and the nitrogen atom in the dimethylamino group. ^{1}H and ^{13}C NMR spectroscopic analyses indicate that the free ligand was obtained as a mixture of two major isomers as shown in Scheme 1 due probably to the stabilizing interaction of the C–H···N hydrogen bond.

Synthesis and characterization of alkyl rare-earth metal complexes 1a and 1b

Alkane elimination reaction of $Sc(CH_2SiMe_3)_3(THF)_2$ or $Y(CH_2SiMe_3)_3(THF)_2$ with 1 eq. of the free ligand **HL** in *n*-hexane at room temperature, followed by a C–H activation of the aminomethyl group as shown in Scheme 2 produced the binuclear alkyl monocyclopentadienyl rare-earth metal complexes $[(C_5Me_4\text{-}C_6H_4\text{-}o\text{-}CH_2N(Me)CH_2\text{-}\mu)Ln(CH_2SiMe_3)]_2$(Ln = Sc (**1a**) and Y (**1b**)) in 74% and 66% isolated yields. Similar intra-molecular C–H activation reaction has been reported in the literature.[5b,14] Complexes **1a** and **1b** were fully characterized by ^{1}H and ^{13}C NMR, IR, elemental analyses, and X-ray crystallographic analysis. The molecular structures of complexes **1a** and **1b**, together with their selected bond distances and angles, are shown in Fig. 1 and 2, respectively. In the ^{1}H NMR spectra, the methylene protons of the NCH_2Sc groups in complex **1a** display two doublet resonances at 1.79 and 2.06 ppm, and those of the NCH_2Y groups in complex **1b** display two doublet resonances at 1.66 and 1.71 ppm, which are slightly different from those in the reported complexes $[(C_5Me_4\text{-}C_6H_4\text{-}o\text{-}N(Me)CH_2\text{-}\mu)Ln(CH_2SiMe_3)]_2$.[5b,14] The methylene protons of the $ArCH_2N$ groups in complexes **1a** and **1b** display resonances of typical doublet of doublets (**1a**: 2.85, 3.82 ppm, J_{H-H} = 14.0 Hz; and **1b**: 2.82, 3.59 ppm, J_{H-H} = 13.6 Hz). X-ray analysis reveals that both complexes **1a** and **1b** adopt a dimeric structure, in which each metal center bonds to one η^5-Me_4Cp unit, one coordinated nitrogen atom, one η^1-CH_2SiMe_3 group, and two carbon atoms of the NCH_2Ln groups. The bond distances (Sc–Cp(av.), 2.522 Å; Sc–CH_2SiMe_3, 2.228(3) Å; Y–Cp (av.), 2.657 Å; and Y–CH_2SiMe_3, 2.368(4) Å) in complexes **1a**

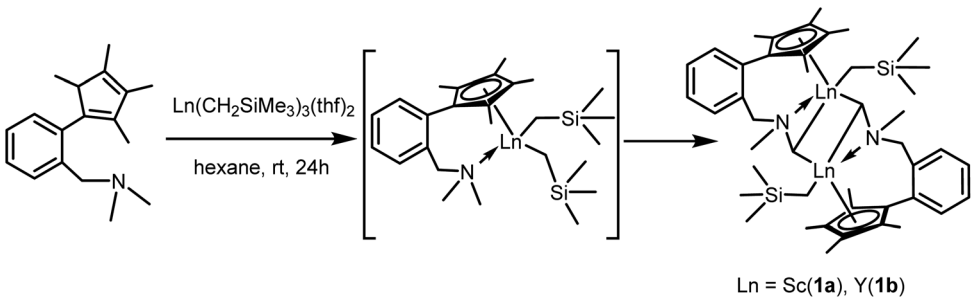

Scheme 2 Synthesis of the alkyl rare-earth metal complexes **1a** and **1b**.

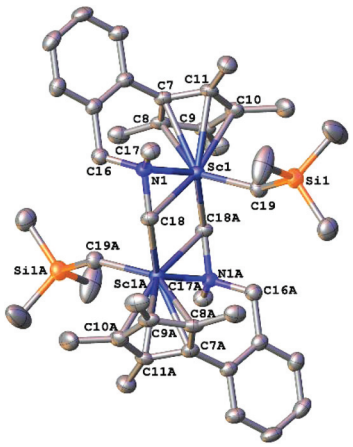

Fig. 1 Perspective view of **1a** with thermal ellipsoids drawn at the 30% probability level. Hydrogen atoms are partially omitted for clarity. Selected bond distances (Å) and angles (°): Sc1–C_{Cp}(av.), 2.522; Sc1–Cp_{cent}, 2.215; Sc1–C18, 2.456(3); Sc1–C19, 2.228(3); Sc1–N1, 2.196(2); Sc1A–C18–N1, 138.86(17); C18–N1–Ln1, 81.06(13); C16–N1–Sc1, 113.81(15); C16–N1–C18, 109.9(2); N1–Sc1–Cp_{cent}, 107.9; C18–Sc1–Cp_{cent}, 140.8; and C19–Sc1–Cp_{cent}, 118.1.

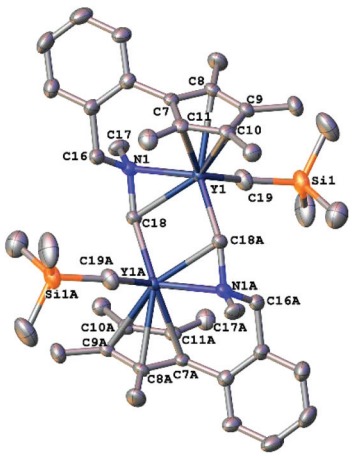

Fig. 2 Perspective view of **1b** with thermal ellipsoids drawn at the 30% probability level. Hydrogen atoms are partially omitted for clarity. Selected bond distances (Å) and angles (°): Y1–C_{Cp}(av.), 2.657; Y1–Cp_{cent}, 2.364; Y1–C18, 2.597(3); Y1–C19, 2.368(4); Y1–N1, 2.352(3); Y1A–C18–N1, 141.0(2); C18–N1–Y1, 81.67(16); C16–N1–Y1, 108.54(19); C16–N1–C18, 109.2(2); N1–Y1–Cp_{cent}, 105.7; C18–Y1–Cp_{cent}, 136.2; and C19–Y1–Cp_{cent}, 117.0.

and **1b** are in agreement with those in the reported complexes $[(C_5Me_4\text{-}C_6H_4\text{-}o\text{-}N(Me)CH_2\text{-}\mu)Ln(CH_2SiMe_3)]_2$ (Sc–Cp(av.), 2.496(2) Å; Sc–CH_2SiMe_3, 2.228(2) Å; Y–Cp(av.), 2.638(2) Å; and Y–CH_2SiMe_3, 2.399(3) Å).[5b,14] Ln–Cp_{cent} bond distances (2.215 Å for **1a** and 2.364 Å for **1b**) are slightly longer than those in $[(C_5Me_4\text{-}C_6H_4\text{-}o\text{-}N(Me)CH_2\text{-}\mu)Ln(CH_2SiMe_3)]_2$ (Sc–Cp_{cent}, 2.186 Å; and Y–Cp_{cent}, 2.347(2) Å).[5b,14] Ln–N bond lengths in complexes **1a** and **1b** (2.196(2) Å and2.352(3) Å, respectively) are shorter than those in $[(C_5Me_4\text{-}C_6H_4\text{-}o\text{-}N(Me)CH_2\text{-}\mu)Ln(CH_2SiMe_3)]_2$(Sc–N, 2.246(2) Å; and Y–N, 2.389(2) Å).[5b,14] In addition, the Cp_{cent}–Ln–N bite angles in complexes **1a** and **1b** (107.9° and 105.7°, respectively) are slightly larger than those found in the complex $[(C_5Me_4\text{-}C_6H_4\text{-}o\text{-}N(Me)CH_2\text{-}\mu)Ln(CH_2SiMe_3)]_2$ (Cp_{cent}–Sc–N, 101.5°; and Cp_{cent}–Y–N, 96.7(3)°).[5b,14]

Synthesis and characterization of dichloro rare-earth metal complexes 2a and 2b

The new dichloro rare-earth metal complexes $(C_5Me_4\text{-}C_6H_4\text{-}o\text{-}CH_2NMe_2)_2Y_2Cl_4[LiCl(THF)_2]$ (**2a**) and $[(C_5Me_4\text{-}C_6H_4\text{-}o\text{-}CH_2NMe_2)LuCl(\mu\text{-}Cl)]_2$ (**2b**) were synthesized in good yields (68% and 72%, respectively) by reactions of the lithium salt of the ligand (Li**L**) with anhydrous yttrium trichloride or lutetium trichloride in THF at room temperature, as shown in Scheme 3. Complexes **2a** and **2b** were fully characterized by ^1H and ^{13}C NMR, IR, elemental analyses, and X-ray crystallographic analysis. In the ^1H NMR spectra, the methylene protons of the $ArCH_2N$ groups in complex **2a** display two broad resonances at 3.05 and 4.71 ppm, while the corresponding methylene protons in complex **2b** display two sets of doublets at 3.09 and 4.74 ppm with a germinal H–H coupling constant of 12.0 Hz. In addition, complex **2a** shows two sets of singlet resonances for the four methyl groups on the Cp ring (2.02 and 2.12 ppm), while complex **2b** shows four sets of singlet resonances (2.06, 2.13, 2.16 and 2.18 ppm) for the corresponding methyl groups. The molecular structures of complexes **2a** and **2b**, together with their selected bond distances and angles, are shown in Fig. 3 and 4, respectively. X-ray diffraction analysis reveals that complex **2a** exists in a hetero-trinuclear structural form connected by multiple μ-Cl bridges in the solid state, which is similar to a known complex $[(C_5Me_4\text{-}C_6H_4\text{-}o\text{-}NMe_2)_2Y_2Cl_4][LiCl(THF)_2]$[9] reported in the literature. The bond lengths of Y1–$Cp1_{cent}$ (2.367 Å) and Y2–$Cp2_{cent}$ (2.379 Å) are longer than the corresponding bonds

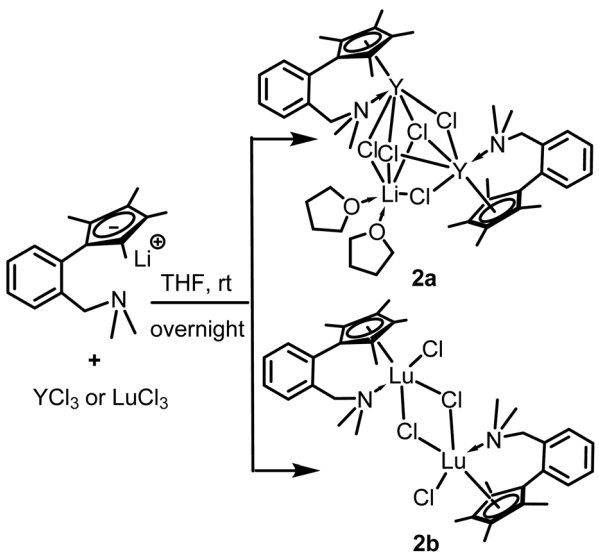

Scheme 3 Synthesis of the dichloro rare-earth metal complexes **2a** and **2b**.

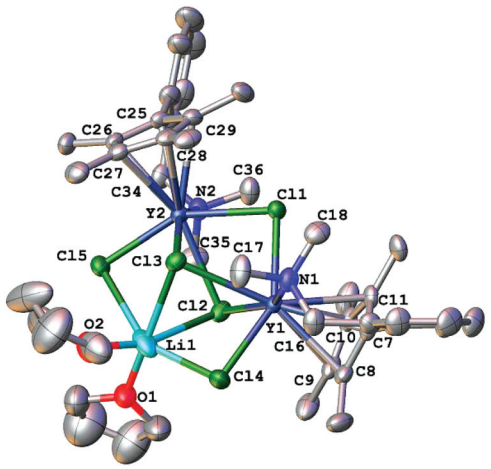

Fig. 3 Perspective view of **2a** with thermal ellipsoids drawn at the 30% probability level. Hydrogen atoms are partially omitted for clarity. Selected bond distances (Å) and angles (°): Y1–C_{Cp1}(av.), 2.656; Y2–C_{Cp2}(av.), 2.669; Y1–$Cp1_{cent}$, 2.367; Y2–$Cp2_{cent}$, 2.379; Y1–N1, 2.557(3); Y2–N2, 2.578(3); Y1–Cl1, 2.7287(10); Y1–Cl2, 2.6945(10); Y1–Cl3, 2.9088(10); Y1–Cl4, 2.6383(10); Y2–Cl1, 2.7609(10); Y2–Cl2, 2.8498(10); Y2–Cl3, 2.6935(10); Y2–Cl5, 2.6111(10); Li–Cl2, 2.811(9); Li–Cl3, 2.556(8); N1–Y1–$Cp1_{cent}$, 101.9; N2–Y2–$Cp2_{cent}$, 103.0; Y1–Cl1–Y2, 93.19(3); Y1–Cl2–Y2, 91.96(3); Y1–Cl3–Y2, 90.69(3); C16–N1–Y1, 109.3(2); and C34–N2–Y2, 111.9(2).

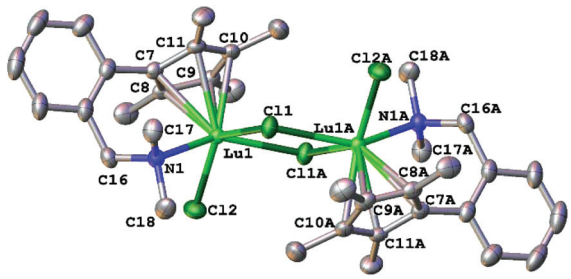

Fig. 4 Perspective view of **2b** with thermal ellipsoids drawn at the 30% probability level. Hydrogen atoms are partially omitted for clarity. Selected bond distances (Å) and angles (°): Lu1–C_{Cp}(av.), 2.572; Lu1–Cp_{cent}, 2.271; Lu1–N1, 2.438(3); Lu1–Cl1, 2.6145(7); Lu1–Cl2, 2.5078(8); N1–Lu1–Cp_{cent}, 105.4; Lu1–Cl1–Lu1A, 103.33(2); C16–N1–Lu1, 107.93(18); N1–Lu1–Cl1, 83.01(6); N1–Lu1–Cl2, 87.59(5); and Cl2–Lu1–Cl1, 129.66(3).

in the complex $[(C_5Me_4\text{-}C_6H_4\text{-}o\text{-}NMe_2)_2Y_2Cl_4][LiCl(THF)_2]$.[9] The Cp_{cent}–Y–N bite angles (N1–Y1–$Cp1_{cent}$, 101.9°; and N2–Y2–$Cp2_{cent}$, 103.0°) in complex **2a** are larger than those observed in $[(C_5Me_4\text{-}C_6H_4\text{-}o\text{-}NMe_2)_2Y_2Cl_4][LiCl(THF)_2]$ (94.6(4)°).[9] In contrast, complex **2b** crystallizes in a simple dimeric form in which the metal centers are bridged symmetrically by two μ-Cl atoms. There is a crystallographic inversion center in the center of the Lu–Cl1A–LuA–Cl1 plane. In complex **2b**, the bond length of Lu–Cp_{cent} (2.271 Å) is shorter than that reported for a similar complex in the literature.[9] The Cp_{cent}–Lu–N bite angle (105.4°) in complex **2b** is larger than the Cp_{cent}–Y–N bite angle in complex **2a** and the one in the related known complex $[(C_5Me_4\text{-}C_6H_4\text{-}o\text{-}NMe_2)_2Lu_2Cl_4][LiCl(THF)_2]$ (95.8(7)°).[9]

Synthesis and characterization of bis(borohydrido) rare-earth metal complexes 3a and 3b

The bis(borohydrido) rare-earth metal complexes $[(C_5Me_4\text{-}C_6H_4\text{-}o\text{-}CH_2NMe_2)Ln(\mu\text{-}BH_4)BH_4]_2$ (Ln = Sm (**3a**) and Nd (**3b**)) were synthesized by reactions of $Ln(BH_4)_3(THF)_3$ (Ln = Sm and Nd) with the lithium salt of the ligand Li**L** in THF at room temperature in good yields (66% and 70% for **3a** and **3b**, respectively), as shown in Scheme 4. Complex **3a** was isolated as an orange color crystalline solid while complex **3b** was obtained as a light blue color crystalline material. Both complexes **3a** and **3b** were found to be air and moisture sensitive, but thermally stable under an inert atmosphere. Both complexes are well soluble in THF, dichloromethane and toluene, but slightly soluble in hexane. The IR spectra of complexes **3a** and **3b** display four strong absorptions in the region between 2200 and 2500 cm^{-1}, being diagnostic of μ^2- and μ^3-coordinated borohydride ligands.[25]

Single crystals of **3a** and **3b** for X-ray diffraction analysis were grown from a mixture of toluene and hexane at −30 °C for several days. The molecular structures of complexes **3a** and **3b**, together with their selected bond distances and angles, are shown in Fig. 5 and 6, respectively. X-ray diffraction analysis

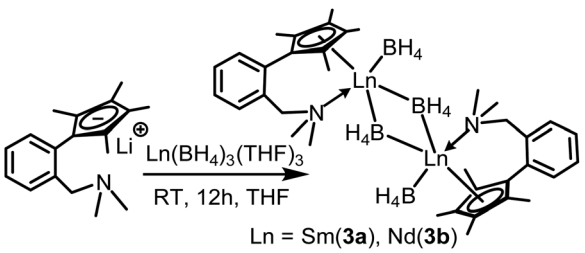

Scheme 4 Synthesis of the bis(borohydrido) rare-earth metal complexes **3a** and **3b**.

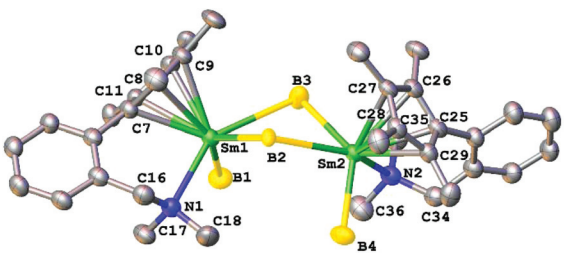

Fig. 5 Perspective view of **3a** with thermal ellipsoids drawn at the 30% probability level. Solvent molecular and hydrogen atoms are partially omitted for clarity. Selected bond distances (Å) and angles (°): Sm1–C_{Cp1}(av.), 2.679; Sm1–$Cp1_{cent}$, 2.391; Sm1–N1, 2.617(7); Sm1–B1, 2.588(11); Sm1–B2, 2.829(7); Sm1–B3, 3.046(11); Sm2–C_{Cp2}(av.), 2.671; Sm2–$Cp2_{cent}$, 2.385; Sm2–N2, 2.602(7); Sm2–B4, 2.603(11); Sm2–B2, 2.939(8); Sm2–B3, 2.896(10); $Cp1_{cent}$–Sm1–N1, 103.3; $Cp1_{cent}$–Sm1–B1, 119.0; $Cp1_{cent}$–Sm1–B2, 110.5; $Cp1_{cent}$–Sm1–B3, 112.3; C16–N1–Sm1, 109.6(5); N1–Sm1–B1, 89.5(3); $Cp2_{cent}$–Sm2–N2, 101.8; $Cp2_{cent}$–Sm2–B4, 114.1; $Cp2_{cent}$–Sm2–B2, 115.8; $Cp2_{cent}$–Sm2–B3, 111.7; C34–N2–Sm2, 112.4(5); N2–Sm2–B4, 92.0(3); Sm1–B2–Sm2, 101.2(2); and Sm1–B3–Sm2, 97.2(3).

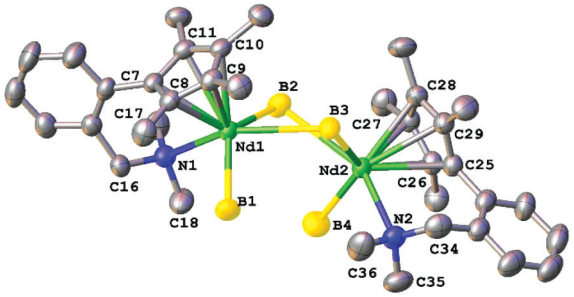

Fig. 6 Perspective view of **3b** with thermal ellipsoids drawn at the 30% probability level. Solvent molecular and hydrogen atoms are partially omitted for clarity. Selected bond distances (Å) and angles (°): Nd1–C_{Cp1}(av.), 2.702; Nd1–$Cp1_{cent}$, 2.422; Nd1–N1, 2.624(3); Nd1–B1, 2.624(5); Nd1–B2, 2.945(5); Nd1–B3, 3.016(5); Nd2–C_{Cp2}(av.), 2.705; Nd2–$Cp2_{cent}$, 2.422; Nd2–N2, 2.637(3); Nd2–B4, 2.629(5); Nd2–B2, 3.078(5); Nd2–B3, 2.878(4); $Cp1_{cent}$–Nd1–N1, 100.7; $Cp1_{cent}$–Nd1–B1, 112.5; $Cp1_{cent}$–Nd1–B2, 119.0; $Cp1_{cent}$–Nd1–B3, 111.4; C16–N1–Nd1, 112.9(2); N1–Nd1–B1, 92.92(14); $Cp2_{cent}$–Nd2–N2, 102.1; $Cp2_{cent}$–Nd2–B4, 117.8; $Cp2_{cent}$–Nd2–B2, 110.5; $Cp2_{cent}$–Nd2–B3, 115.0; C34–N2–Nd2, 111.3(2); N2–Nd2–B4, 89.85(15); Nd1–B2–Nd2, 95.85(14); and Nd1–B3–Nd2, 98.66(13).

reveals that both complexes **3a** and **3b** exist in a dimeric form with the two central metal atoms being bridged by two μ-(BH_4) units in the solid state. In complexes **3a** and **3b**, the Ln–B (terminal BH_4 group) bond lengths (Sm1–B1, 2.588(11) Å; Sm2–B4, 2.603(11) Å; Nd1–B1, 2.624(5) Å; and Nd2–B4, 2.629(5) Å) are noticeably shorter than the Ln–B (μ^2-bridging BH_4 group) bond lengths (Sm1–B2, 2.829(7) Å; Sm1–B3, 3.046(11) Å; Sm2–B2, 2.939(8) Å; Sm2–B3, 2.896(10) Å; Nd1–B2, 2.945(5) Å; Nd1–B3, 3.016(5) Å; Nd2–B2, 3.078(5) Å; and Nd2–B3, 2.878(4) Å). The Ln–N bond lengths are only slightly different (Sm1–N1, 2.617(7) Å; Sm2–N2, 2.602(7) Å; Nd1–N1, 2.624(3) Å; and Nd2–N2, 2.637(3) Å). The Ln–Cp_{cent} bond lengths (Sm1–$Cp1_{cent}$, 2.391 Å; Sm2–$Cp2_{cent}$, 2.385 Å; Nd1–$Cp1_{cent}$, 2.422 Å; and Nd2–$Cp2_{cent}$, 2.422 Å) are comparable to those in the related complexes $[(C_5H_3{}^tBu_2)_2Sm(\mu\text{-}BH_4)]_2$ (2.46 Å),[23a] [Cp*′Sm$(BH_4)_2$(thf)] (2.456 Å)[23b] and [Cp*′Sm{(*p*-tol)NN}(BH_4)]$_2$ (2.430 Å).[24a] The Cp_{cent}–Ln–N bite angles of these two complexes ($Cp1_{cent}$–Sm1–N1, 103.3°; $Cp2_{cent}$–Sm2–N2, 101.8°; $Cp1_{cent}$–Nd1–N1, 100.7°; and $Cp2_{cent}$–Nd2–N2, 102.1°) are close.

Polymerization of isoprene

Polymerization reactions of isoprene with the alkyl rare earth metal complexes **1a** and **1b** as precatalysts were investigated under different conditions. The representative results are summarized in Table 1. Upon activation with 1 equiv. of $Ph_3CB(C_6F_5)_4$, both complexes **1a** and **1b** show catalytic activity for the polymerization of isoprene with or without the presence of excess AlR_3. The neutral complexes **1a** and **1b** alone were found to be inactive for the polymerization of isoprene, suggesting that the generation of a cationic alkyl metal species is essential for the polymerization reaction. It was found that the **1a**/$Ph_3CB(C_6F_5)_4$ and **1b**/$Ph_3CB(C_6F_5)_4$ binary catalyst systems show much lower catalytic activity than the **1a**/AlR_3/$Ph_3CB(C_6F_5)_4$ and **1b**/AlR_3/$Ph_3CB(C_6F_5)_4$ ternary catalyst systems, although both catalytic systems demonstrate almost the same high *cis*-1,4 selectivity (up to 92.6%) (entries 1–4 in Table 1). $B(C_6F_5)_3$ was also tested as the activator in the ternary catalytic systems, while no detectable polymer was obtained from the polymerization reaction (entry 12 in Table 1). The scandium- and yttrium-based catalyst systems show similar catalytic activity under similar conditions while the yttrium-based catalyst system exhibits slightly higher *cis*-1,4 selectivity than the corresponding scandium-based catalyst system (entries 1–4 in Table 1), which might reveal that the larger ionic radius of yttrium (1.040 Å) in complex **1b** is beneficial for the *cis*-η^4 coordination of the isoprene monomer.[26,27] The type of trialkylaluminum was found to have apparent influences on

Table 1 Results of isoprene polymerization using **1a** and **1b** as catalyst precursors[a]

Entry	Cat.	IP/Cat.	AlR_3	*t* (h)	Conv. (%)	M_n [b] (×10^4)	M_w/M_n [b]	Macrostructure[c] *cis*-1,4/*trans*-1,4/3,4-
1	**1a**	2000	—	2	48	13.4	3.12	90.5/0/9.5
2	**1b**	2000	—	2	47	14.6	2.67	92.6/0/7.4
3	**1a**	2000	Al^iBu_3	0.5	76	10.5	3.22	90.1/0/9.9
4	**1b**	2000	Al^iBu_3	0.5	79	11.5	1.79	92.6/0/7.4
5	**1b**	2000	$AlEt_3$	0.5	68	9.87	2.34	87.2/0/12.8
6	**1b**	2000	$AlMe_3$	12	54	7.84	2.56	82.4/0/17.6
7	**1b**	1000	Al^iBu_3	0.5	83	10.6	1.76	92.2/0/7.8
8	**1b**	3000	Al^iBu_3	0.5	63	14.9	2.44	93.6/0/6.4
9[d]	**1b**	2000	Al^iBu_3	0.5	66	13.2	2.38	92.2/0/7.8
10[e]	**1b**	2000	Al^iBu_3	0.5	39	6.79	3.65	90.5/0/9.5
11[f]	**1b**	2000	Al^iBu_3	12	16	18.7	1.87	95.5/0/4.5
12[g]	**1b**	2000	Al^iBu_3	12	Trace	—	—	—
13[h]	**1b**	2000	—	0.5	66	6.21	2.78	88.5/0/11.5
14[i]	**1b**	2000	—	0.5	73	10.4	2.61	89.6/0/10.4
15[j]	**2a**	2000	Al^iBu_3	12	Trace	—	—	—
16[j]	**2b**	2000	Al^iBu_3	12	Trace	—	—	—

[a] Conditions: 5 μmol Cat., 5 μmol $Ph_3CB(C_6F_5)_4$, 5 mL of C_6H_5Cl, AlR_3/Cat. = 5 : 1, 20 °C. [b] Measured by GPC calibrated with the standard polystyrene samples. [c] Determined by ^1H NMR and ^{13}C NMR. [d] Al/Cat. = 2.5 : 1. [e] Al/Cat. = 10 : 1. [f] The polymerization temperature was −20 °C. [g] $B(C_6F_5)_3$ was used instead of $Ph_3CB(C_6F_5)_4$. [h] Activated by 1000 equiv. of MAO. [i] Activated by 1000 equiv. of MMAO. [j] Al^iBu_3/Cat. = 60 : 1.

the catalytic activity and the *cis*-1,4 selectivity of the ternary catalyst systems. The $AlMe_3$-containing catalyst system shows lower catalytic activity than the $AlEt_3$- and Al^iBu_3-containing catalyst systems, and the Al^iBu_3-containing catalyst system shows the highest *cis*-1,4 selectivity (up to 92.6%) among these ternary catalyst systems (entries 4–6 in Table 1). The influences of the monomer/catalyst molar ratio on the conversion of the monomer and the molecular weight of the polymer products in the ternary catalyst systems were also examined and it was found that an increase in the monomer/catalyst molar ratio from 1000 to 3000 leads to a corresponding decrease in the conversion of the monomer and increase in the polymer molecular weight (entries 4, 7 and 8 in Table 1). The influences of the Al^iBu_3/catalyst molar ratio (from 2.5/1 to 10/1) on the conversion of the monomer and the molecular weight of the polymer products in the ternary catalyst systems were also investigated. It was found that an increase in the Al^iBu_3/catalyst molar ratio results in a decrease in the polymer molecular weight (entries 4, 9 and 10 in Table 1), while the highest conversion of the monomer was observed at the Al^iBu_3/catalyst molar ratio of 5/1 under similar conditions. In addition, a polymerization reaction with the **1b**/Al^iBu_3/$Ph_3CB(C_6F_5)_4$ catalyst system carried out at −20 °C produced a polyisoprene sample with a relatively high *cis*-1,4 selectivity of 95.5% and a number-averaged molecular weight of 18.7×10^4 Dalton (entry 11 in Table 1). The above mentioned results are similar to those reported for the related similar catalyst systems, while the *cis*-1,4 selectivity and number-averaged molecular weight of the polyisoprenes obtained with our catalyst systems are obviously higher than those observed with the reported $[(C_5Me_4\text{-}C_6H_4\text{-}o\text{-}N(Me)CH_2\text{-}\mu)Sc(CH_2SiMe_3)]_2$/$Ph_3CB(C_6F_5)_4$ catalyst systems,[5b] due probably to bulkier coordination environment in complexes **1a** and **1b** than in the complex $[(C_5Me_4\text{-}C_6H_4\text{-}o\text{-}N(Me)CH_2\text{-}\mu)Sc(CH_2SiMe_3)]_2$, which would weaken the interaction between the cationic active catalyst and the anionic cocatalyst and therefore favor the coordination of isoprene to the catalyst in *cis*-1,4 fashion. We also investigated the polymerization reactions of isoprene using MAO and MMAO activated catalyst systems **1b**/MAO and **1b**/MMAO. It was found that the **1b**/MAO and **1b**/MMAO binary catalyst systems show slightly lower catalytic activity and *cis*-1,4 selectivity than the **1b**/AlR_3/$Ph_3CB(C_6F_5)_4$ ternary catalyst system under similar conditions (entries 13 and 14 in Table 1). The dichloro rare-earth metal complexes **2a** and **2b** were also tested as precatalysts for the isoprene polymerization reaction using the **2a**/AlR_3/$Ph_3CB(C_6F_5)_4$ and **2b**/AlR_3/$Ph_3CB(C_6F_5)_4$ ternary catalyst systems. However, no polymer was obtained.

Attempts to isolate the catalytically active species from the binary catalyst system **1a**/$Ph_3CB(C_6F_5)_4$ and the ternary catalyst system **1a**/2Al^iBu_3/$Ph_3CB(C_6F_5)_4$ were not successful. Fortunately, monitoring the reaction mixtures of both catalyst systems by ^1H, ^{11}B, and ^{19}F NMR spectroscopy in *o*-dichlorobenzene-d_4 (*o*-$C_6D_4Cl_2$) provided some information on the catalytically active species and the possible catalyst activation procedure. As seen in ^1H NMR spectra shown in Fig. S17 in the ESI,† the disappearance of signals for the methylene protons (at −0.64 and −1.14 ppm) of Sc–CH_2SiMe_3 and the appearance of $Ph_3CCH_2SiMe_3$ and Ph_3CH in the ^1H NMR spectrum of the **1a**/$Ph_3CB(C_6F_5)_4$ reaction mixture indicate the abstraction of the alkyl group Me_3SiCH_2 from **1a** by the trityl cation and the formation of the catalytically active cationic species $[C_5Me_4\text{-}C_6H_4\text{-}o\text{-}CH_2NMe(CH_2\text{-}\mu)]Sc^+$. Similar observations on the formation of the catalytically cationic species[28] and the organic byproducts Ph_3CH and an unknown Me_3Si-containing compound[29] have previously been reported. In the ternary catalyst system **1a**/Al^iBu_3/$Ph_3CB(C_6F_5)_4$, the formation of Ph_3CH and $CH_2{=}CMe_2$ was observed from the reaction mixture of Al^iBu_3 and $Ph_3CB(C_6F_5)_4$, which suggests that the activation of the catalyst system starts with the abstraction of a β-H of the Al^iBu_3 by the Ph_3C^+ cation to form a $^iBu_2Al^+$ cation, along with the production of Ph_3CH and $CH_2{=}CMe_2$ as shown in Scheme 5. The $^iBu_2Al^+$ cation can further react with the precatalyst **1a** to produce the catalytically active species $[C_5Me_4\text{-}C_6H_4\text{-}o\text{-}CH_2NMe(CH_2\text{-}\mu)]Sc^+$ and $^iBu_2AlCH_2SiMe_3$. The ^{11}B and ^{19}F NMR spectra of these reaction mixtures remain similar to those observed for $Ph_3CB(C_6F_5)_4$, suggesting the presence of only one type of anion $B(C_6F_5)_4^-$.

Polymerization of 1-hexene

Polymerization reactions of 1-hexene with the rare earth metal alkyl complexes **1a** and **1b** as precatalysts were investigated under different conditions. The polymerization results are summarized in Table 2. The **1a**/$Ph_3CB(C_6F_5)_4$ and **1b**/$Ph_3CB(C_6F_5)_4$ binary catalyst systems were found to show low catalytic activity for the 1-hexene polymerization reaction. Upon activation with AlR_3/$Ph_3CB(C_6F_5)_4$ (R = Me, Et, and ^{i}Bu), complexes **1a** and **1b** both show moderate catalytic activity for 1-hexene polymerization in neat monomer. Under similar conditions, the chloride and borohydride rare earth metal complexes **2a**, **2b**, **3a** and **3b** were also tested for the polymerization of 1-hexene and found to be inactive even in the presence of 300 μmol Al^iBu_3 at 40 °C for 24 h. The reason for the inactivity of **2a**, **2b**, **3a** and **3b** is unclear. The influence of the type of AlR_3 on the catalytic activity of the **1b**/AlR_3/$Ph_3CB(C_6F_5)_4$ catalyst systems was examined, and the catalytic activity of these catalyst systems was found to increase in the order of $AlMe_3$ < $AlEt_3$ < Al^iBu_3 (entries 4–6 in Table 2). The 1-hexene polymerization experiments using the **1b**/Al^iBu_3/$Ph_3CB(C_6F_5)_4$ catalyst system at different polymerization temperatures (0, 20, 40 and 60 °C) were also carried out, and an increase in the catalytic

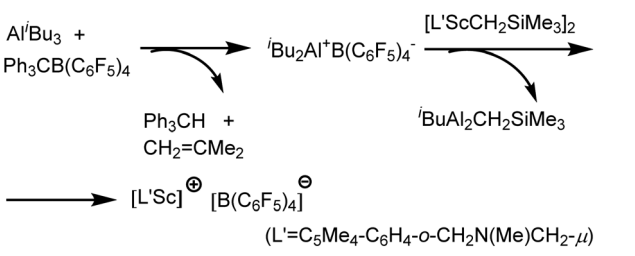

Scheme 5 A possible mechanism for the catalyst activation procedure.

Table 2 Results of 1-hexene polymerization using **1a** and **1b** as precursors[a]

Entry	Cat.	AlR_3	T (°C)	t (h)	Yield (g)	M_n [b] ($\times 10^4$)	M_w/M_n [b]
1	**1a**	—	20	24	Trace	—	—
2	**1b**	—	20	24	Trace	—	—
3	**1a**	Al^iBu_3	20	12	1.02	9.57	1.78
4	**1b**	Al^iBu_3	20	12	1.04	10.9	1.69
5	**1b**	$AlEt_3$	20	12	0.76	8.69	1.46
6	**1b**	$AlMe_3$	20	12	0.44	8.53	1.48
7	**1b**	Al^iBu_3	0	12	0.52	16.0	1.56
8	**1b**	Al^iBu_3	40	12	1.12	6.32	1.51
9	**1b**	Al^iBu_3	60	12	1.05	5.12	1.43
10[c]	**1b**	—	20	12	0.82	4.21	1.67
11[d]	**1b**	—	20	12	0.98	8.22	1.64

[a] Conditions: 5 μmol Cat., 5 μmol $Ph_3CB(C_6F_5)_4$, 5 mL (3.4 g) of 1-hexene, AlR_3/Cat. = 10 : 1. [b] Determined by GPC calibrated with the standard polystyrene samples. [c] Activated by 1000 equiv. of MAO. [d] Activated by 1000 equiv. of MMAO.

activity of this catalyst system with an increase in the polymerization temperature was observed (entries 4, 7, 8 and 9 in Table 2). ^{13}CNMR spectroscopic analysis[30,31] of the poly(1-hexene) samples indicates that atactic poly(1-hexene)s were obtained with the **1a**/AlR_3/$Ph_3CB(C_6F_5)_4$ and **1b**/AlR_3/$Ph_3CB(C_6F_5)_4$ catalyst systems. It has been known that half-sandwich scandium(III) complexes without a side arm catalyze the atactic polymerization of 1-hexene,[32,33] while C_s-symmetric half-sandwich scandium(III) complexes with a coordinating imine side arm produce isotactic poly(1-hexene)s (with [*mmmm*] up to 95%).[6] The ^{13}C NMR spectrum of a typical poly(1-hexene) sample is given in Fig. S16 (see the ESI†). The lack of olefinic resonances in both the ^{1}H and ^{13}C NMR spectra of the obtained poly(1-hexene)s[30] suggests that the chain-transfer to alkylaluminum, rather than the β-H elimination, is the main chain termination process in these polymerization reactions. The GPC analysis of the polymer products reveals that the poly(1-hexene)s produced by these catalyst systems possess moderate molecular weights (M_n = 5.12–16.0 × 10^4 g mol^{-1}). In addition, the **1b**/MAO and **1b**/MMAO catalyst systems both were found to exhibit slightly lower catalytic activity and molecular weight than the **1b**/AlR_3/$Ph_3CB(C_6F_5)_4$ ternary catalyst system under similar conditions.

Polymerization of MMA

We also investigated the catalytic properties of the rare earth metal complexes **1a**, **1b**, **2a**, **2b**, **3a** and **3b** for the polymerization reaction of MMA. It was found that the alkyl and chloride complexes **1a**, **1b**, **2a** and **2b** show no catalytic activity even in the presence of ^{n}BuLi, $^iBu_3Al$, $B(C_6F_5)_3$, $Ph_3CB(C_6F_5)_4$, ^{n}BuLi/$B(C_6F_5)_3$ or ^{n}BuLi/$Ph_3CB(C_6F_5)_4$ and even after a long reaction time, while the borohydrido complexes **3a** and **3b** show moderate catalytic activity for the polymerization of MMA. The results of MMA polymerisation experiments are summarised in Table 3. Under similar conditions, the samarium complex **3a** was found to exhibit higher catalytic reactivity than the neodymium complex **3b**. The same order of catalytic activity has been reported in similar MMA polymerization systems with samarium and neodymium complexes as catalysts.[34,35] Polymerization reactions of neat MMA without any cocatalyst

Table 3 Results of MMA polymerization using **3a** and **3b** as precursors[a]

Entry	Cat.	Co-cat.	Solvent	T (°C)	t (min)	Conv.[b] (%)	M_n [c] ($\times 10^4$)	M_w/M_n [c]	Tacticity[d] (%) mm-mr-rr
1	**3a**	—	—	20	10	79.2	1.23	2.35	24-41-35
2	**3b**	—	—	20	10	58.0	1.33	3.12	51-28-21
3	**3a**	—	Tol	20	240	9.3	1.03	1.87	51-35-14
4	**3a**	—	Tol	0	240	34.5	1.77	2.79	51-31-18
5	**3b**	—	Tol	20	240	5.7	1.06	1.78	60-31-9
6	**3b**	—	Tol	0	240	28.4	2.00	3.96	56-32-12
7	**3a**	—	THF	20	30	69.6	3.30	2.03	6-32-62
8	**3b**	—	THF	20	240	77.6	1.36	1.79	6-34-60
9[e]	**3b**	—	THF	20	240	72.6	1.54	1.84	7-38-55
10[f]	**3b**	—	THF	20	240	57.4	1.61	1.77	12-39-48
11	**3a**	^{n}BuLi	Tol	20	30	13.1	1.02	1.73	60-32-8
12	**3a**	^{n}BuLi	THF	20	30	71.4	1.11	1.82	6-36-58
13	**3a**	^{n}BuLi	THF	0	30	60.0	2.93	1.94	6-31-63
14	**3a**	^{n}BuLi	THF	−20	15	73.1	4.99	1.86	3-26-71
15	**3a**	^{n}BuLi	THF	−40	5	76.3	7.52	2.44	3-24-73
16	**3b**	^{n}BuLi	THF	20	90	61.2	1.24	1.75	7-36-57
17	**3b**	^{n}BuLi	THF	0	60	81.8	2.42	1.83	6-32-62
18	**3b**	^{n}BuLi	THF	−20	30	72.7	5.34	3.56	4-29-67
19	**3b**	^{n}BuLi	THF	−40	30	77.8	5.75	2.14	4-28-68
20	**3a**	Me_3SiCH_2Li	THF	20	30	70.6	1.22	1.88	7-32-61
21	**3a**	MeLi	THF	20	30	71.8	1.13	1.93	5-35-60
22	**3a**	^{i}PrMgBr	THF	20	30	70.2	1.28	2.01	5-34-61
23	**3a**	^{n}BuLi	Et_2O	20	30	62.6	1.26	1.70	8-37-55
24	**3a**	^{n}BuLi	Dioxane	20	30	71.1	1.29	1.86	6-34-60

[a] Conditions: Cat. (10 μmol), solvent (1 mL), [MMA]/[Cat.] = 500, [^{n}BuLi]/[Cat.] = 3. [b] Conversion = weight of polymer obtained/weight of monomer used. [c] Determined by GPC calibrated with the standard polystyrene samples. [d] Determined by ^{1}H NMR spectroscopy in $CDCl_3$ (mm: isotactic triad rate; mr: atactic triad rate; and rr: syndiotactic triad rate). [e] [MMA]/[Cat.] = 800. [f] [MMA]/[Cat.] = 1000.

exhibited high monomer conversion and afforded atactic polymer products (entries 1 and 2 in Table 3). When the polymerization reactions were performed in THF, polymers with relatively high rr triad content (entry 7 in Table 3) were obtained in high monomer conversion. In contrast, polymerization reactions of MMA in toluene produced polymers with relatively high mm triad content in low monomer conversion (entries 3–6 in Table 3). The effects of the monomer/catalyst molar ratio on the monomer conversion and the polymer molecular weight were examined for the **3b** catalyst system. As expected, it was observed that the monomer conversion decreases and the molecular weight of the produced PMMA increases with an increase in the MMA/**3b** molar ratio (entries 8–10 in Table 3). Generally speaking, the monomer conversion and syndio-selectivity in the polymerization reactions of MMA catalyzed by **3a** and **3b** in THF are higher than or comparable to those reported for similar MMA polymerization reactions using samarium and neodymium borohydride complexes as catalysts.[36] The polymerization reactions of MMA were also studied using **3a**/^{n}BuLi and **3b**/^{n}BuLi binary catalyst systems in toluene or THF. The monomer conversion in the reactions with these binary catalyst systems improved moderately in comparison with those observed in the unitary catalyst systems. With the binary catalyst systems, the mm triad contents in the polymers obtained from the polymerization reactions of MMA in toluene are slightly higher and the rr triad contents in the polymers obtained from the polymerization reactions of MMA in THF are slightly lower than those observed in the unitary catalyst systems (entries 3, 7, 8, 11, 12 and 16 in Table 3). In addition, the rr triad contents in the polymers obtained from the polymerization reactions of MMA using the binary catalyst systems increase with a decrease in the polymerization temperature (entries 12–19 in Table 3). Considering that the possible reaction[37] between ^{n}BuLi and THF may interfere with the MMA polymerization reaction, the MMA polymerization experiments in THF using other lithium and magnesium alkyls (Me_3SiCH_2Li, MeLi and ^{i}PrMgCl) as cocatalysts were also carried out. It was observed that under similar conditions the monomer conversions and the rr triad contents in the formed polymers are comparable to those observed in the reactions using ^{n}BuLi as the cocatalyst (entries 20–22 in Table 3). These results demonstrate that the possible reactions between lithium alkyls and THF seem to show little effect on the MMA polymerization reaction, and the lithium or magnesium alkyls might only play a role of scavenging agents in the polymerization reaction. To further clarify the influence of the potential ^{n}BuLi/THF reaction on the MMA polymerization, the MMA polymerization reactions were also carried out in diethyl ether and dioxane. The observed monomer conversion and syndio-selectivity from the reaction in dioxane are comparable with those obtained in the polymerization reaction in THF, while the monomer conversion and syndio-selectivity from the reaction in diethyl ether are both lower than those seen in the polymerization reaction in THF due probably to relatively low polarity of diethyl ether (entries 23 and 24 in Table 3).

Conclusions

A new *ortho*-dimethylaminomethylphenyl-tetramethylcyclopentadiene ligand precursor C_5Me_4H-C_6H_4-*o*-CH_2NMe_2 (**HL**) and a series of rare-earth metal complexes bearing this ligand have been developed. The binuclear alkyl scandium and yttrium complexes **1a** and **1b** were synthesized by the alkane elimination reactions of the free ligand with $Sc(CH_2SiMe_3)_3(THF)_2$ and $Y(CH_2SiMe_3)_3(THF)_2$, respectively, followed by an intramolecular C–H activation process of a NMe group in the ligand with a CH_2SiMe_3 group. The dichlorido complexes of yttrium and lutetium **2a** and **2b** were synthesized by reactions of the lithium salt of the ligand with the corresponding anhydrous rare earth metal chloride. The bis(borohydrido) complexes of samarium and neodymium **3a** and **3b** were obtained by reactions of the lithium salt of the ligand with $Sm(BH_4)_3(THF)_3$ and $Nd(BH_4)_3(THF)_3$, respectively. The binuclear alkyl complexes **1a** and **1b** show good catalytic activity for isoprene *cis*-1,4 enriched regioselective polymerization and moderate catalytic activity for 1-hexene polymerization upon activation with AlR_3/$Ph_3CB(C_6F_5)_4$, MAO or MMAO. Complexes **3a** and **3b** show moderate to high catalytic activity for methyl methacrylate polymerization reaction.

Experimental section

General methods and materials

All manipulations involving air- and/or moisture-sensitive compounds were carried out under a nitrogen atmosphere (ultra-high purity) using either the standard Schlenk techniques or glove box techniques. Toluene, diethyl ether, dioxane and THF were distilled under a nitrogen atmosphere in the presence of sodium and benzophenone; *n*-hexane was refluxed over CaH_2 distilled under a nitrogen atmosphere. All solvents were stored over 4 Å molecular sieves. Methyl methacrylate (MMA), ^{n}BuLi (2.5 M in hexane), *N*,*N*-dimethylbenzylamine, ^{i}PrMgCl (2 M in THF), MeLi (1.6 M in diethyl ether), 2,3,4,5-tetramethylcyclopent-2-enone and $NaBH_4$ were purchased from Aldrich. Isoprene, 1-hexene and methyl methacrylate (MMA) were first degassed and dried over CaH_2 under stirring for 48 h and distilled under vacuum before use. Me_3SiCH_2Li,[38] $Ln(CH_2SiMe_3)_3(thf)_n$,[39] $Ln(BH_4)_3(THF)_n$,[16] $B(C_6F_5)_3$[40] and $Ph_3CB(C_6F_5)_4$[41] were prepared according to the literature. Elemental analyses were performed using a Varian EL microanalyzer. Infrared spectra were recorded using KBr disks with a Nicolet Avatar 360. The ^{1}H and ^{13}C NMR spectra of the ligand and complexes were recorded using a Bruker Avance III-400 NMR spectrometer. The microstructure of the polymer was determined by its ^{1}H and ^{13}C NMR spectra, which were obtained with a Bruker Avance III-400 NMR spectrometer. The chemical shifts were referenced to residual $CHCl_3$ in the solvent (δ = 7.26 ppm). The polymer number-average molecular weight (M_n) and molecular weight distributions ($Đ = M_w/M_n$) were measured by gel permeation chromatography (GPC) at 35 °C and at a flow rate of 1 mL min^{-1},

with THF (HPLC grade) as an eluent using a Waters 1515 instrument equipped with a guard column MIXED 7.5 × 50 mm PL column and two MIXED-C 7.5 × 300 columns and a differential refractive index detector.

Synthesis of *N*,*N*-dimethyl-1-(2-(2,3,4,5-tetramethylcyclopenta-1,3-dienyl)phenyl)methanamine (HL)

N,*N*-Dimethylbenzylamine (27.0 g, 0.200 mol) in anhydrous diethyl ether (100 mL) was treated with *n*-butyllithium (2.50 mol L^{-1}, 80 mL) in hexane under a N_2 atmosphere. The reaction mixture was refluxed for 30 h with stirring, and then cooled to room temperature. 2,3,4,5-Tetramethylcyclopent-2-enone (27.6 g, 0.200 mol) was added dropwise over 30 min so as to bring the solution to a gentle reflux and the mixture was refluxed for 2 h. The solution was cooled in an ice-bath and hydrochloric acid (6 mol L^{-1}, 150 mL) was carefully added. It was then concentrated under reduced pressure to give a red syrup which was redissolved in water (100 mL) and the pH was adjusted to 10 by adding 10 mol L^{-1} sodium hydroxide solution. The product then separated as a yellow oil, which was removed and the aqueous layer was extracted with diethyl ether (3 × 50 mL). The combined organic phase was dried over anhydrous $MgSO_4$, filtered, then concentrated using a rotary evaporator and finally vacuum distilled to yield a yellow viscous oil at 100–110 °C/10^{-2} mbar (28.1 g, 0.111 mol, 55.4%). ^{1}H NMR ($CDCl_3$, 400 MHz, 298 K): δ 0.90–1.91 (m, 12H, Cp*Me*), 2.14–2.23 (m, 6H, N*Me*$_2$), 2.67–3.52 (m, 3H, ArC*H*$_2$ and Cp*H*), 6.99–7.67 (m, 4H, Ar*H*) ppm. ^{13}C NMR ($CDCl_3$, 100 MHz, 298 K): δ 11.13, 11.22, 11.64, 11.86, 12.01, 12.47, 14.31, 14.54 (Cp*Me*), 45.48, 45.49 (N*Me*$_2$), 51.59, 51.92 (Cp*C*H), 60.66, 60.76 (Ar*C*H$_2$), 125.58, 126.32, 126.42, 126.95, 127.62, 128.75, 129.09, 129.60, 129.84, 130.55, 133.96, 134.17, 137.15, 137.90, 138.22, 139.17, 139.82, 140.04, 140.45, 140.60 (aromatics and Cp ring carbons) ppm.

Synthesis of complex [(C_5Me_4-C_6H_4-*o*-$CH_2N(Me)CH_2$-μ)Sc(CH_2SiMe_3)]$_2$ (1a)

To a *n*-hexane (3 mL) solution of Sc(CH_2SiMe_3)$_3$(thf)$_2$ (0.451 g, 1.00 mmol), 1 equiv. of HL (0.255 g, 1.00 mmol) in *n*-hexane (2 mL) was added dropwise at room temperature. After the reaction mixture was stirred for 24 h, the volatiles were removed under vacuum, affording a yellow oily residue which was recrystallized from *n*-hexane at −30 °C to give complex **1a** as a colorless crystalline solid (0.262 g, 0.340 mmol, 73.6%). Single crystals for X-ray analysis were grown from *n*-hexane over several days at −30 °C. ^{1}H NMR (C_6D_6, 400 MHz, 298 K): δ −1.00 (d, *J* = 10.8 Hz, 2H, C*H*$_2$SiMe$_3$), −0.50 (d, *J* = 10.8 Hz, 2H, C*H*$_2$SiMe$_3$), 0.21 (s, 18H, CH$_2$Si*Me*$_3$), 1.67 (s, 6H, Cp*Me*), 1.79 (d, *J* = 12.8 Hz, 2H, NC*H*$_2$), 2.03 (s, 6H, Cp*Me*), 2.06 (d, *J* = 12.8 Hz, 2H, NC*H*$_2$), 2.14 (s, 6H, Cp*Me*), 2.20 (s, 6H, Cp*Me*), 2.47 (s, 6H, N*Me*), 2.85 (d, *J* = 14.0 Hz, 2H, ArC*H*$_2$), 3.82 (d, *J* = 14.0 Hz, 2H, ArC*H*$_2$), 6.96–7.05 (m, 8H, Ar*H*) ppm. ^{13}C NMR (C_6D_6, 100 MHz, 298 K): δ 4.91 (s, CH$_2$Si*Me*$_3$), 12.29 (s, Cp*Me*), 12.37 (s, Cp*Me*), 13.06 (s, Cp*Me*), 13.29 (s, Cp*Me*), 33.92 (s, *C*H$_2$SiMe$_3$), 34.13 (s, *C*H$_2$SiMe$_3$), 49.29 (s, N*Me*), 64.17 (s, ArCH$_2$), 69.08 (s, NCH$_2$), 115.24, 118.36, 120.55, 121.23, 122.77, 127.04, 128.87, 129.98, 132.78, 135.66, 137.98 (aromatics and Cp ring carbons) ppm. IR (KBr): 3695 (w), 2953 (s), 2908 (s), 2864 (s), 2785 (w), 1599 (m), 1454 (s), 1379 (m), 1248 (s), 1028 (w), 987 (w), 860 (s), 760 (m), 696 (w). Anal. calcd (%) for $C_{44}H_{68}N_2Si_2Sc_2$ (771.10): C, 68.53; H, 8.89; N, 3.63. Found: C, 68.32; H, 8.68; N, 3.55.

Synthesis of complex [(C_5Me_4-C_6H_4-*o*-$CH_2N(Me)CH_2$-μ)Y(CH_2SiMe_3)]$_2$ (1b)

Following a similar procedure described for the preparation of **1a**, complex **1b** was isolated from the reaction of Y(CH_2SiMe_3)$_3$(thf)$_2$ (0.495 g, 1.00 mmol) with 1 equiv. of HL (0.255 g, 1.00 mmol) in a 66.2% yield (0.284 g, 0.331 mmol) as starting materials. Pure **1b** was obtained as a white crystalline solid. Single crystals for X-ray analysis were grown from *n*-hexane at −30 °C within several days. ^{1}H NMR (C_6D_6, 400 MHz, 298 K): δ −1.14 to −1.11 (dd, *J*1 = 14.4 Hz, *J*2 = 2.4 Hz, 2H, C*H*$_2$SiMe$_3$), −0.58 to −0.55 (dd, *J*1 = 14.4 Hz, *J*2 = 2.4 Hz, 2H, C*H*$_2$SiMe$_3$), 0.23 (s, 18H, CH$_2$Si*Me*$_3$), 1.66 (d, *J* = 13.2 Hz, 2H, NC*H*$_2$), 1.71 (d, *J* = 13.2 Hz, 2H, NC*H*$_2$), 1.78 (s, 6H, Cp*Me*), 2.06 (s, 6H, Cp*Me*), 2.07 (s, 6H, Cp*Me*), 2.15 (s, 6H, Cp*Me*), 2.45 (s, 6H, N*Me*), 2.82 (d, *J* = 13.6 Hz, 2H, ArC*H*$_2$), 3.59 (d, *J* = 13.6 Hz, 2H, ArC*H*$_2$), 6.95–7.18 (m, 8H, Ar*H*) ppm. ^{13}C NMR (C_6D_6, 100 MHz, 298 K): δ 4.86 (s, CH$_2$Si*Me*$_3$), 11.54 (s, Cp*Me*), 12.06 (s, Cp*Me*), 12.19 (s, Cp*Me*), 12.57 (s, Cp*Me*), 38.99 (s, *C*H$_2$SiMe$_3$), 39.44 (s, *C*H$_2$SiMe$_3$), 45.59, 47.64 (s, 2C, N*Me*), 64.28 (s, 2C, Ar*C*H$_2$), 68.43 (d, *J*(Y,C) = 24.0 Hz, 1C, Ar*C*H$_2$), 68.74 (d, *J*(Y,C) = 24.0 Hz, 1C, N*C*H$_2$), 116.25, 118.07, 118.15, 119.66, 121.37, 126.90, 129.16, 130.75, 133.50, 135.52, 138.51 (aromatics and Cp ring carbons) ppm. IR (KBr): 3682 (w), 2955 (s), 2910 (s), 2858 (s), 1597 (m), 1552 (s), 1444 (s), 1377 (m), 1250 (m), 858 (s), 758 (m), 700 (w). Anal. calcd (%) for $C_{44}H_{68}N_2Si_2Y_2$ (859.02): C, 61.52; H, 7.98; N, 3.26. Found: C, 61.34; H, 7.79; N, 3.18.

Synthesis of complex (C_5Me_4-C_6H_4-*o*-CH_2NMe_2)$_2Y_2Cl_4$[LiCl(THF)$_2$] (2a)

Under a nitrogen atmosphere, to a solution of the free ligand HL (0.255 g, 1.00 mmol) in 20 mL of THF was added dropwise a solution of *n*-BuLi (2.50 mol L^{-1}, 0.400 mL, 1.00 mmol) in *n*-hexane at −78 °C. The reaction mixture was warmed to room temperature and stirred for 2 h. The resulting solution was then added dropwise to a THF suspension (20 mL) of YCl_3 (0.195 g, 1.00 mmol) at room temperature and the reaction mixture was stirred overnight. Removing the volatiles under reduced pressure, extracting the residue with toluene and evaporating toluene to dryness afforded **2a** as a white crystalline solid (0.346 g, 0.341 mmol, 68.2%). Single crystals for X-ray analysis were grown from a mixture of toluene and hexane at −30 °C within several days. ^{1}H NMR ($CDCl_3$, 400 MHz, 298 K): δ 1.90 (br s, 8H, THF), 1.90 (br s, 6H, N*Me*$_2$), 2.02 (br s, 12H, Cp*Me*), 2.12 (br s, 12H, Cp*Me*), 2.86 (br s, 6H, N*Me*$_2$), 3.05 (br s, 2H, ArC*H*$_2$), 3.90 (br s, 8H, THF), 4.71 (br s, 2H, ArC*H*$_2$), 7.16 (d, *J* = 7.5 Hz, 2H, Ar*H*), 7.25–7.29 (m, *J* = 16.0 Hz, 4H, Ar*H*), 7.35–7.39 (m, *J* = 16.2 Hz, 2H, Ar*H*) ppm. ^{13}C NMR ($CDCl_3$, 100 MHz, 298 K): δ 12.07 (s, 4C, Cp*Me*), 12.89 (s, 4C, Cp*Me*),

25.44(s, 4C, THF), 53.35 (s, 4C, NMe_2), 66.48 (s, 2C, ArCH_2), 68.84(s, 4C, THF), 120.66, 122.09, 122.92, 126.54, 128.64, 131.70, 132.81, 133.91, 137.18 (aromatics and Cp ring carbons) ppm. IR (KBr): 2972 (m), 2906 (s), 2864 (m), 2727 (w), 1601 (w), 1508 (m), 1472 (s), 1454 (s), 1410 (w), 1379 (m), 1306 (w), 1148 (w), 1022 (m), 986 (m), 953 (m), 827 (m), 758 (s), 737 (m). Anal. calcd (%) for $C_{44}H_{64}Cl_5LiN_2O_2Y_2$ (1014.98): C, 52.07; H, 6.36; N, 2.76. Found: C, 51.94; H, 6.31; N, 2.68.

Synthesis of complex [(C_5Me_4-C_6H_4-*o*-CH_2NMe_2)LuCl(μ-Cl)]$_2$ (2b)

Following a similar procedure described for the preparation of **2a**, complex **2b** was isolated with compounds $LuCl_3$ (0.281 g, 1.00 mmol), *n*-BuLi (2.50 mol L^{-1}, 0.400 mL, 1.00 mmol) and H**L** (0.255 g, 1.00 mmol) in a 72.3% yield (0.362 g, 0.362 mmol) as starting materials. Pure **2b** was obtained as a white crystalline solid. Single crystals for X-ray analysis were grown from a mixture of toluene and hexane at −30 °C within several days. ^{1}H NMR ($CDCl_3$, 400 MHz, 298 K): δ 1.97 (s, 6H, NMe_2), 2.06 (s, 6H, Cp*Me*), 2.13 (s, 6H, Cp*Me*), 2.16 (s, 6H, Cp*Me*), 2.18 (s, 6H, Cp*Me*), 2.74 (s, 6H, NMe_2), 3.09 (d, J = 12.0 Hz, 2H, ArCH_2), 4.74 (d, J = 12.0 Hz, 2H, ArCH_2), 7.11 (d, J = 7.3 Hz, 2H, Ar*H*), 7.27–7.31 (m, 4H, Ar*H*), 7.36–7.40 (m, 2H, Ar*H*). ^{13}C NMR ($CDCl_3$, 100 MHz, 298 K): δ 11.98 (s, 4C, Cp*Me*), 12.17 (s, 4C, Cp*Me*), 53.56 (s, 4C, NMe_2), 65.09 (s, 2C, ArCH_2), 114.72, 117.52, 122.84, 126.54, 128.32, 131.23, 133.40, 135.86, 137.73 (aromatics and Cp ring carbons). IR (KBr): 3022 (w), 2966 (s), 2918 (s), 2862 (s), 2723 (w), 1659 (m), 1634 (m), 1506 (m), 1475 (s), 1448 (s), 1408 (w), 1379 (m), 1018 (m), 987 (m), 953 (m), 827 (m), 760 (s), 739 (m). Anal. calcd (%) for $C_{36}H_{48}Cl_4N_2Lu_2$ (1000.50): C, 43.22; H, 4.84; N, 2.80. Found: C, 43.05; H, 4.79; N, 2.68.

Synthesis of complex [(C_5Me_4-C_6H_4-*o*-CH_2NMe_2)Sm(μ-BH_4)BH_4]$_2$ (3a)

Under a nitrogen atmosphere, to a solution of the free ligand H**L** (0.255 g, 1.00 mmol) in 20 mL of THF was added dropwise a solution of *n*-BuLi (2.50 mol L^{-1}, 0.400 mL, 1.00 mmol) in *n*-hexane at −78 °C. The reaction mixture was warmed to room temperature and stirred for 2 h. The resulting solution was then added dropwise to a THF suspension (20 mL) of Sm$(BH_4)_3(THF)_3$ (0.411 g, 1.00 mmol) at room temperature and the reaction mixture was stirred overnight. Removing the volatiles under reduced pressure, extracting the residue with toluene and evaporating toluene to dryness afforded **3a** as an orange solid (0.286 g, 0.329 mmol, 65.8%). Single crystals for X-ray analysis were grown from a mixture of toluene and hexane at −30 °C within several days. IR (KBr): 2964 (m), 2912 (s), 2860 (s), 2432 (s), 2386 (m), 2291 (s), 2223 (s), 1599 (w), 1470 (m), 1379 (w), 1306 (w), 1169 (s), 1124 (s), 1020 (w), 986 (w), 955 (w), 829 (m), 760 (m), 735 (m), 696 (w). Anal. calcd (%) for $C_{36}H_{64}B_4N_2Sm_2$ (868.83): C, 49.76; H, 7.42; N, 3.22. Found: C, 49.51; H, 7.28; N, 3.08.

Synthesis of complex [(C_5Me_4-C_6H_4-*o*-CH_2NMe_2)Nd(μ-BH_4)BH_4]$_2$ (3b)

Following a similar procedure described for the preparation of **3a**, complex **3b** was isolated with compounds $Nd(BH_4)_3(THF)_3$ (0.405 g, 1.00 mmol), *n*-BuLi (2.50 mol L^{-1}, 0.400 mL, 1.00 mmol) and H**L** (0.255 g, 1.00 mmol) in a 70.2% yield (0.301 g, 0.351 mmol) as starting materials. Pure **3b** was obtained as a light-blue crystalline solid. Single crystals for X-ray analysis were grown from a mixture of toluene and hexane at −30 °C within several days. IR (KBr): 2964 (m), 2912 (s), 2860 (m), 2432 (s), 2386 (s), 2291 (s), 2226 (s), 1599 (w), 1470 (m), 1379 (w), 1308 (w), 1169 (s), 1124 (s), 1022 (w), 986 (w), 955 (w), 829 (m), 760 (m), 735 (m), 696 (w). Anal. calcd (%) for $C_{36}H_{64}B_4N_2Nd_2$ (856.61): C, 50.48; H, 7.53; N, 3.27. Found: C, 50.26; H, 7.38; N, 3.06.

X-ray crystallographic studies

Single crystals of complexes suitable for X-ray analysis were obtained by recrystallization from hexane or a mixture of toluene and hexane (v/v = 1–2 : 10). The crystals were mounted on glass fibers using an oil drop. Data obtained in the ω–2θ scan mode were collected using a Bruker SMART 1000 CCD diffractometer equipped with a graphite-monochromated Mo Kα radiation source (λ = 0.71073 Å). The structures were solved using direct methods, and further refinements with full-matrix least squares on F^2 were performed using the SHELXTL program package. All non-hydrogen atoms were refined anisotropically. Hydrogen atoms were introduced in the calculated positions with the displacement factors of the host carbon atoms. All calculations were performed using the SHELXTL crystallographic software package.[42] The structures of **3a** and **3b** contain disordered solvent molecules. Attempts to obtain a suitable disorder model failed. Accordingly the SQUEEZE of the PLATON program was used to obtain a new set of $F^2(hkl)$ values without the contribution of solvent molecules, leading to the presence of significant voids in these structures.[43]

Crystal data for 1a. $C_{44}H_{68}N_2Si_2Sc_2$, M_r = 771.10, a = 9.8597(8) Å, b = 15.9005(13) Å, c = 14.3669(12) Å, α = 90°, β = 106.9240(10)°, γ = 90°, V = 2154.8(3) Å^3, space group $P2(1)/c$, Z = 2, $\mu(Mo_{K\alpha})$ = 0.402 mm^{-1}, 12 144 reflections measured, and 4398 independent reflections (R_{int} = 0.0380). The final R_1 = 0.0507 and wR_2 = 0.1268 ($I > 2\delta$). The goodness of fit on F^2 was 1.037.

Crystal data for 1b. $C_{44}H_{68}N_2Si_2Y_2$, M_r = 859.00, a = 9.2689(6) Å, b = 11.0330(8) Å, c = 11.9125(8) Å, α = 77.1150(10)°, β = 75.8990(10)°, γ = 72.1310(10)°, V = 1109.92(13) Å^3, space group $P\bar{1}$, Z = 1, $\mu(Mo_{K\alpha})$ = 2.686 mm^{-1}, 6334 reflections measured, and 4409 independent reflections (R_{int} = 0.0146). The final R_1 = 0.0329 and wR_2 = 0.0915 ($I > 2\delta$). The goodness of fit on F^2 was 1.206.

Crystal data for 2a. $C_{44}H_{64}Cl_5LiN_2O_2Y_2$, M_r = 1014.98, a = 20.3069(12) Å, b = 10.5790(6) Å, c = 24.3769(15) Å, α = 90°, β = 111.2640(10)°, γ = 90°, V = 4880.3(5) Å^3, space group $P2(1)/c$, Z = 4, $\mu(Mo_{K\alpha})$ = 2.675 mm^{-1}, 27 203 reflections measured, and 9957 independent reflections (R_{int} = 0.0343). The final R_1 = 0.0426 and wR_2 = 0.1144 ($I > 2\delta$). The goodness of fit on F^2 was 1.052.

Crystal data for 2b. $C_{36}H_{48}Cl_4Lu_2N_2$, M_r = 1000.50, a = 12.5958(8) Å, b = 24.8514(15) Å, c = 12.0503(7) Å, α = 90°, β = 90°, γ = 90°, V = 3772.0(4) Å^3, space group $Pccn$, Z = 4, $\mu(Mo_{K\alpha})$ = 1.762 mm^{-1}, 20 140 reflections measured, and 3863 independent reflections (R_{int} = 0.0387). The final R_1 = 0.0214 and wR_2 = 0.0514 ($I > 2\delta$). The goodness of fit on F^2 was 1.043.

Crystal data for 3a. $C_{36}H_{64}B_4N_2Sm_2$, M_r = 868.83, a = 8.6992(5) Å, b = 12.4170(7) Å, c = 21.8057(12) Å, α = 92.1500°, β = 94.7390(10)°, γ = 96.5830(10)°, V = 2329.3(2) Å^3, space group $P\bar{1}$ Z = 2, $\mu(Mo_{K\alpha})$ = 2.518 mm^{-1}, 13 240 reflections measured, and 9200 independent reflections (R_{int} = 0.0186). The final R_1 = 0.0360 and wR_2 = 0.0989 ($I > 2\delta$). The goodness of fit on F^2 was 1.102.

Crystal data for 3b. $C_{36}H_{48}B_4N_2Nd_2$, M_r = 856.61, a = 8.732(6) Å, b = 22.278(14) Å, c = 24.533(16) Å, α = 90°, β = 99.094(11)°, γ = 90°, V = 4712(5) Å^3, space group $P2_1/c$, Z = 4, $\mu(Mo_{K\alpha})$ = 2.200 mm^{-1}, 26 636 reflections measured, and 9621 independent reflections (R_{int} = 0.0265). The final R_1 = 0.0292 and wR_2 = 0.0710 ($I > 2\delta$). The goodness of fit on F^2 was 1.027.

Isoprene polymerization

In the glovebox, to a mixture of C_6H_5Cl, isoprene, and procatalyst was added a mixture of AlR_3 (5 equiv.)/$Ph_3CB(C_6F_5)_4$ (1 equiv.) at polymerization temperature. The contents of the flask were stirred for a determined time. Methanol was injected to terminate the polymerization. The reaction mixture was poured in methanol with vigorous stirring, leading to the precipitation of the polymer which was filtered and dried at 40 °C under vacuum to a constant weight.

Neat 1-hexene polymerization

In the glovebox, AlR_3 (5 equiv.) and $Ph_3CB(C_6F_5)_4$ (1 equiv.) were dissolved in 1 mL of 1-hexene and added to a stirred solution of the corresponding complexes in 1-hexene (4 mL). The resulting mixture was stirred until the resulting polymer solution had become viscous. Methanol was injected to terminate the polymerization. The reaction mixture was poured in methanol with vigorous stirring, leading to the precipitation of the polymer which was filtered and dried at 40 °C under vacuum to a constant weight.

Polymerization of MMA

A flask equipped with a magnetic stirring bar, to which were added the catalyst and the solvent, was then placed in a thermostatic bath. After some time, the polymerization was started by direct addition of monomer to the catalyst solution by means of a syringe. The contents of the flask were stirred for a determined time. Methanol was injected to terminate the polymerization. The reaction mixture was poured in methanol with vigorous stirring, leading to the precipitation of the polymer which was filtered and dried at 40 °C under vacuum to a constant weight.

Conflicts of interest

The authors declare no competing financial interest.

Acknowledgements

We are grateful for the financial support from the National Natural Sciences Foundation of China (51673078 and U1462111).

Notes and references

1 (*a*) A. A. Trifonov and D. M. Lyubov, *Coord. Chem. Rev.*, 2017, **340**, 10; (*b*) Y. Nakayama and H. Yasuda, *J. Organomet. Chem.*, 2004, **689**, 4489; (*c*) J. Gromada, J.-F. Carpentier and A. Mortreux, *Coord. Chem. Rev.*, 2004, **248**, 397; (*d*) M. Zimmermann and R. Anwander, *Chem. Rev.*, 2010, **110**, 6194; (*e*) H. Yasuda, *J. Organomet. Chem.*, 2002, **647**, 128; (*f*) J.-F. Carpentier, S. M. Guillaume, E. Kirillov and Y. Sarazin, *C. R. Chim.*, 2010, **13**, 608; (*g*) W. E. Piers and D. J. H. Emslie, *Coord. Chem. Rev.*, 2002, **233–234**, 131; (*h*) F. T. Edelmann, D. M. M. Freckmann and H. Schumann, *Chem. Rev.*, 2002, **102**, 1851.

2 (*a*) S. Arndt and J. Okuda, *Chem. Rev.*, 2002, **102**, 1953; (*b*) P. M. Zeimentz, S. Arndt, B. R. Elvidge and J. Okuda, *Chem. Rev.*, 2006, **106**, 2404; (*c*) Z. Hou, *Bull. Chem. Soc. Jpn.*, 2003, **76**, 2253; (*d*) G. A. Molander and J. A. C. Romero, *Chem. Rev.*, 2002, **102**, 2161; (*e*) H. Schumann, J. A. Meese-Marktscheffel and L. Esser, *Chem. Rev.*, 1995, **95**, 865.

3 (*a*) M. Nishiura, F. Guo and Z. Hou, *Acc. Chem. Res.*, 2015, **48**, 2209; (*b*) J. Okuda, *Dalton Trans.*, 2003, 2367.

4 L. N. Jende, C. O. Hollfelder, C. Maichle-Mössmer and R. Anwander, *Organometallics*, 2015, **34**, 32.

5 (*a*) L. Zhang, Y. Luo and Z. Hou, *J. Am. Chem. Soc.*, 2005, **127**, 14562; (*b*) X. Li, M. Nishiura, L. Hu, K. Mori and Z. Hou, *J. Am. Chem. Soc.*, 2009, **131**, 13870.

6 X. Tao, W. Gao, H. Huo and Y. Mu, *Organometallics*, 2013, **32**, 1287.

7 D. J. Beetstra, A. Meetsma, B. Hessen and J. H. Teuben, *Organometallics*, 2003, **22**, 4372.

8 I. L. Fedushkin, S. Dechert and H. Schumann, *Organometallics*, 2000, **19**, 4066.

9 Z. Jian, W. Zhao, X. Liu, X. Chen, T. Tang and D. Cui, *Dalton Trans.*, 2010, **39**, 6871.

10 Z. Jian, D. Cui, Z. Hou and X. Li, *Chem. Commun.*, 2010, **46**, 3022.

11 Z. Jian, S. Tang and D. Cui, *Chem. –Eur. J.*, 2010, **16**, 14007.

12 Z. Jian, S. Tang and D. Cui, *Macromolecules*, 2011, **44**, 7675.

13 Z. Jian, A. R. Petrov, N. K. Hangaly, S. Li, W. Rong, Z. Mou, K. A. Rufanov, K. Harms, J. Sundermeyer and D. Cui, *Organometallics*, 2012, **31**, 4267.

14 Z. Jian, D. Cui and Z. Hou, *Chem. –Eur. J.*, 2012, **18**, 2674.

15 Y. Pan, W. Rong, Z. Jian and D. Cui, *Macromolecules*, 2012, **45**, 1248.

16 S. M. Cendrowski-Guillaume, G. L. Gland, M. Nierlich and M. Ephritikhine, *Organometallics*, 2000, **19**, 5654.

17 P. Zinck, A. Valente, A. Mortreux and M. Visseaux, *Polymer*, 2007, **48**, 4609.

18 M. Visseaux, P. Zinck, M. Terrier, A. Mortreux and P. Roussel, *J. Alloys Compd.*, 2008, **451**, 352.

19 D. B.-Baudry, F. Bouyer, A. S. M. Bruno and M. Visseaux, *Appl. Organomet. Chem.*, 2006, **20**, 24.

20 F. Bonnet, C. D. C. Violante, P. Roussel, A. Mortreux and M. Visseaux, *Chem. Commun.*, 2009, 3380.

21 A. Valente, P. Zinck, A. Mortreux and M. Visseaux, *Macromol. Rapid Commun.*, 2009, **30**, 528.
22 J. Richter and F. T. Edelmann, *Eur. J. Solid State Inorg. Chem.*, 1996, **33**, 1063.
23 (*a*) Y. K. Gun'ko, B. M. Bulychev, G. L. Soloveichik and V. K. Belsky, *J. Organomet. Chem.*, 1992, **424**, 289; (*b*) H. Schumann, M. R. Keitsch, J. Demtschuk and S. Muhle, *Z. Anorg. Allg. Chem.*, 1998, **624**, 1811.
24 (*a*) F. Bonnet, M. Visseaux, D. B.-Baudry, E. Vigier and M. M. Kubicki, *Chem. – Eur. J.*, 2004, **10**, 2428; (*b*) F. Bonnet, M. Visseaux, D. B.-Baudry, A. Hafid, E. Vigier and M. M. Kubicki, *Inorg. Chem.*, 2004, **43**, 3682.
25 (*a*) T. J. Marks and J. R. Kolb, *Chem. Rev.*, 1977, **77**, 263; (*b*) M. Ephritikhine, *Chem. Rev.*, 1997, **97**, 2193.
26 L. Zhang, T. Suzuki, Y. Luo, M. Nishiura and Z. Hou, *Angew. Chem., Int. Ed.*, 2007, **46**, 1909.
27 L. Li, C. Wu, D. Liu, S. Li and D. Cui, *Organometallics*, 2013, **32**, 3203.
28 (*a*) G. Zhang, S. Wang, X. Zhu, S. Zhou, Y. Wei, Z. Huang and X. Mu, *Organometallics*, 2017, **36**, 3812; (*b*) G. Zhang, B. Deng, S. Wang, Y. Wei, S. Zhou, X. Zhu, Z. Huang and X. Mu, *Dalton Trans.*, 2016, **45**, 15445; (*c*) G. Zhang, S. Wang, S. Zhou, Y. Wei, L. Guo, X. Zhu, L. Zhang, X. Gu and X. Mu, *Organometallics*, 2015, **34**, 4251.
29 (*a*) Y. Pan, T. Xu, Y.-S. Ge and X.-B. Lu, *Organometallics*, 2011, **30**, 5687; (*b*) P. D. Bolton, E. Clot, N. Adams, S. R. Dubberley, A. R. Cowley and P. Mountford, *Organometallics*, 2006, **25**, 2806; (*c*) M. Zimmermann, K. W. Törnroos, R. M. Waymouth and R. Anwander, *Organometallics*, 2008, **27**, 4310; (*d*) Y. Pan, W. Li, N.-N. Wei, Y.-M. So, Y. Li, K. Jiang and G. He, *Dalton Trans.*, 2019, **48**, 3583.
30 G. N. Babu, R. A. Newmark and J. C. W. Chien, *Macromolecules*, 1994, **27**, 3383.
31 T. Asakura, M. Demura and Y. Nishiyama, *Macromolecules*, 1991, **24**, 2334.
32 Z. Hou, Y. Luo and X. Li, *J. Organomet. Chem.*, 2006, **691**, 3114.
33 Y. Luo and Z. Hou, *Stud. Surf. Sci. Catal.*, 2006, **161**, 95.
34 L. Y. Zhou, H. T. Sheng, Y. M. Yao, Y. Zhang and Q. Shen, *J. Organomet. Chem.*, 2007, **692**, 2990.
35 T. J. Woodman, M. Schormann and M. Bochmann, *Organometallics*, 2003, **22**, 2938.
36 (*a*) F. Bonnet, A. C. Hillier, A. Collins, S. R. Dubberley and P. Mountford, *Dalton Trans.*, 2005, 421; (*b*) F. Yuan, Y. Zhu and L. Xiong, *J. Organomet. Chem.*, 2006, **691**, 3377; (*c*) G. G. Skvortsov, M. V. Yakovenko, G. K. Fukin, A. V. Cherkasov and A. A. Trifonov, *Russ. Chem. Bull.*, 2007, **56**, 1742.
37 P. Stanetty and M. D. Mihovilo, *J. Org. Chem.*, 1997, **62**, 1514.
38 H. L. Lewis and T. L. Brown, *J. Am. Chem. Soc.*, 1970, **92**, 4664.
39 M. F. Lappert and R. Pearce, *J. Chem. Soc., Chem. Commun.*, 1973, 126.
40 (*a*) M. Lehmann, A. Schulz and A. Villinger, *Angew. Chem., Int. Ed.*, 2009, **48**, 7444; (*b*) M. Karsch, H. Lund, A. Schulz, A. Villinger and K. Voss, *Eur. J. Inorg. Chem.*, 2012, **4**, 5542; (*c*) A. G. Massey and A. J. Park, *J. Organomet. Chem.*, 1964, **2**, 245.
41 J. C. W. Chien, W. M. Tsai and M. D. Rausch, *J. Am. Chem. Soc.*, 1991, **113**(22), 8570.
42 *SMART and SAINT software packages*, Siemens Analytical X-ray instruments, Inc., Madison, WI, 1996.
43 A. L. Spek, *Acta Crystallogr., Sect. C: Struct. Chem.*, 2015, **71**, 9.